A Tracking Algorithm for Autonomous Navigation of AGVs in an Automated Container Terminal

Yong-Shik Kim
Department of Mechanical and Intelligent Systems Engineering, Pusan National University, San 30 Jangjeon-dong Gumjeong-gu, Busan 609-735, Korea
Keum-Shik Hong*
School of Mechanical Engineering, Pusan National University, San 30 Jangjeon-dong Gumjeong-gu, Busan 609-735, Korea

In this paper, a tracking algorithm for the autonomous navigation of the automated guided vehicles (AGVs) operated in a container terminal is investigated. The navigation system is based on sensors that detect range and bearing. The navigation algorithm used is an interacting multiple model algorithm to detect other AGVs and avoid obstacles using information obtained from the multiple sensors. In order to detect other AGVs (or obstacles), two kinematic models are derived : A constant velocity model for linear motion and a constant-speed turn model for curvilinear motion. For the constant-speed turn model, an unscented Kalman filter is used because of the drawbacks of the extended Kalman filter in nonlinear systems. The suggested algorithm reduces the root mean squares error for linear motions and rapidly detects possible turning motions.

Key Words : Automated Guided Vehicle, Hybrid, Interacting Multiple Model, Nonlinear Filtering, Extended Kalman Filter, Unscented Filter, Navigation

Nomenclature

a : Augmented value
$f[k-1, x(k-1)]$: Nonlinear vector-valued function at time $k-1$
$f^{a}_{x_i^a(k)}$: Jacobian matrix
$G(k)$: Noise transition matrix
$g[k-1, x(k-1)]$: Nonlinear vector-valued function at time k-1
H : Measurement matrix
$h[k, x(k)]$: Nonlinear measurement function
$K(k)$: Kalman filter gain
M : Set of modal state
$m(k)$: Scalar-valued modal state at time k
$P\{\cdot\}$: Probability
P_x : Covariance of x
p : Nonlinear transformation
$Q(k)$: Process noise covariance
$R(k)$: Measurement noise covariance
W_i : Weights of sigma points
$w(k)$: Measurement noise sequence
$x(k)$: System base state vector at time k
$\bar{x}$: Mean of x
$z(k)$: Noisy measurement vector at time k
$\xi(k)$, $\eta(k)$: Orthogonal coordinates of the horizontal plane
κ : Scaling parameter
μ_j : Mode probability
$\nu^{(k-1)}$: Process noise sequence
π_{ij} : Model transition probability
χ_i : Sigma points
$\omega(k)$: Yaw rate at time k
$\Im_i$: Measurement sigma point

* Corresponding Author,
E-mail : kshong@pusan.ac.kr
TEL : +82-51-510-2454; **FAX** : +82-51-514-0685
School of Mechanical Engineering, Pusan National University, San 30 Jangjeon-dong Gumjeong-gu, Busan 609-735, Korea. (Manuscript **Received** May 25, 2004; **Revised** September 30, 2004)

1. Introduction

Recent advances in electronics, sensors, information technologies, and automation have made the operation of a fully automated container terminal technically feasible (Ioannou et al., 2001). The port of Rotterdam is operating a fully automated container terminal, ECT (European Combined Terminal), using automated guided vehicles (AGVs) and automated yard cranes to handle containers, whereas the port of Singapore, Thamesport of England, and the port of Hamburg are experimenting with similar ideas.

The AGV is a vehicle that is driven by an automatic control system that takes the role of the driver. Sensors on the road/vehicle or infrastructure provide measurements about the location and speed of the vehicle, which are used by the automatic control system to generate the appropriate commands for the throttle/brake actuators in order to follow certain position and speed trajectories. AGVs are considered to be the most flexible type of material handling system. Their size ranges from small load carriers of a few kilograms to over 125-ton transporters. The vehicles' working environment ranges from small offices with carpet floor to huge harbor dockside areas.

In container terminals, AGVs are used to replace the manually driven trucks that transport containers within the terminal. Figure 1 shows an AGV, with a load, in the ECT terminal in Rotterdam. In this application, AGVs are automated industrial trucks, which can be powered by electric motors and batteries or by conventional diesel engines. While the automation of vehicles and trucks on highways does not have the strong support of manufacturers due to liability issues and the complexity of the environment in which they have to operate, the use of automated trucks at low speeds in restricted areas such as a terminal or a warehouse is a completely different story. The low speed characteristics of AGVs together with the restricted area they operate in make the overall problem much simpler to solve. Therefore, the use of AGVs as container- handling devices in terminals is feasible from the point of view of technology, and has the strong potential to improve efficiency and save labor costs.

Fig. 1 An AGV in the automated container terminal of ECT at Rotterdam

An AGV system consists of a vehicle, an onboard controller, a management system, a communication system, and a navigation system. The navigation system provides guidance and navigation to the AGV in the operating environment. The guidance and navigation can be based on a fixed-path or a free-path approach.

In the fixed-path approach, the movement of an AGV is restricted to following a fixed path, and there is no flexibility in changing the guide-path. Examples of fixed paths include rail tracks, embedded wires, or other types of guide-ways. In the free-path method, the path of an AGV can be changed dynamically. The system is autonomous and is capable of detecting the path using online information, obstacle detection and collision avoidance systems.

The effectiveness of a navigation system depends on the interpretation of the information arriving from sensors, which provide details of the surrounding environment and obstacles. In particular, all these systems rely on the detection and subsequent tracking of objects around the AGV. Such detection information is provided by radar, lidar, laser scanner, and vision sensor. Before a controller can make a decision that enables the AGV to navigate autonomously, the motion of the surrounding object must be properly interpreted from the available sensor information.

Many studies on the autonomous navigation and localization of AGVs have appeared in the literature. Adam et al.(1999) presented a method of determining the position and orientation of an AGV by fusing odometry with the information provided by a vision system. Zhang et al. (2000) introduced a novel navigation sensor using a position-sensitive detector to direct the vehicle along a predefined trajectory. The navigation sensor mounted on the vehicle picks up signals from floor marks and gives commands to make the vehicle perform linear or turning motions. As well, Park et al.(2002) proposed a path-generation algorithm that uses the sensor scanning method. The scanning algorithm is used to recognize the ambient environment surrounding the AGV, which uses the information from the sensor platform. In (Lee et al., 2002), a land navigation system using global positioning system and reduced reckoning system was used. Lim and Kang (2002) investigated a technique for localization of a mobile robot by using sonar sensors. Localization is the continual provision of knowledge of position that are deduced from it's a priori position estimation. Lee and Yi (2002) represented an investigation of a vehicle-to-vehicle distance control system using hardware-in-the-loop simulation (HiLS). HiLS method is useful in the investigation of driver assistance and active safety systems. Moon and Yi (2002) presented the implementation and vehicle tests of a vehicle longitudinal control scheme for stop and go cruise control. The control scheme consists of a vehicle-to-vehicle distance control algorithm and throttle/brake control algorithm for acceleration tracking. Xu et al.(2003) developed a safe, practical, and dynamic obstacle avoidance method for AGVs. Jin et al.(2003) investigated a sensor fusion technique for AGV navigation. A natural landmark navigation algorithm was utilized for autonomous vehicles operating in relatively unstructured environments in (Madhavan and Durrant-Whyte, 2004).

This paper describes the design of a tracking algorithm for the navigation of an AGV for transporting cargo containers in a port environment. In particular, in order for an AGV to navigate autonomously, a maneuvering-vehicle tracking algorithm for detecting other AGVs (or obstacles) and avoiding a collision, is derived.

The ability to accurately predict the motion of other AGVs (or obstacles) in the terminal environment can improve the controller's ability to adapt smoothly to the behavior of those AGVs (or obstacles) preceding it. This ability to predict motions is dependent on how well the sensors of an AGV can detect other AGVs (or obstacles). In order to detect other AGVs or avoid obstacles using the object information obtained from multiple sensors, tracking techniques based on the Bayesian approach are usually used (Bar-Shalom et al., 2001). The tracking of a maneuvering target is already well-established in the target tracking literature.

Techniques for tracking maneuvering targets are used in many tracking and surveillance systems as well as in applications where reliability is the main concern (Bar-Shalom et al., 2001; Farina, 1999; Houles and Bar-Shalom, 1989; Li and Bar-Shalom, 1993; 1996; Lee, 2003). In particular, tracking a maneuvering target using multiple models can provide better performance than using a single model. Efforts in developing multiple-model algorithms have shown that significant gains in performance are possible using multiple models. A number of multiple model techniques to track a maneuvering target have been proposed in the literature: the multiple-model algorithm (Li and Bar-Shalom, 1996), the interacting multiple models (IMM) algorithm (Bar-Shalom et al., 2001; Li and Bar-Shalom, 1993; Mazor et al., 1998; Simeonova and Semerdjiev, 2002; Lee et al., 2003; Kim and Hong, 2004), the adaptive IMM (Efe and Atherton, 1996; Efe et al., 1999; Jilkov et al., 1999; Munnir and Atherton, 1995), the fuzzy IMM (Ding et al., 2001; McGinnity and Irwin, 1998), the adaptive Kalman filter (Efe et al., 1999), and others.

Generally, target motion models can be divided into two subcategories: the uniform motion model and the maneuvering model. A maneuvering target moving at a constant turn-rate and speed is usually modeled as a maneuvering model, and called a coordinated turn model (Bar-Shalom et

al., 2001 ; Dufour and Mariton, 1992 ; Efe and Atherton, 1996 ; Helferty, 1996 ; Jilkov et al., 1999 ; Li and Bar-Shalom, 1993 ; McGinnity and Irwin, 1998). For application to air traffic control, a fixed structure IMM algorithm with a single constant velocity model and two coordinated turn models was analyzed (Li and Bar-Shalom, 1993). And, for the tracking of a maneuvering target, a validation method of a new type of flight mode was presented in (Nabaa and Bishop, 2000). Nabaa and Bishop (2000) validated a non-constant speed coordinated-turn aircraft maneuver model by comparing their model with the classic Singer maneuver model and a constant-speed coordinated turn model using actual trajectories. Semerdjiev and Mihaylova (2000) discussed variable- and fixed-structure augmented IMM algorithms, whereas a fixed-structure algorithm only was discussed in (Li and Bar-Shalom, 1993), and applied to a maneuvering ship tracking problem by augmenting the turn rate error.

The drawbacks of the augmented IMM algorithm using extended Kalman filters (AIMM-EKF) are as follows : First, the EKF approximates a non-Gaussian density with a Gaussian one (Katsikas et al., 1995 ; Tam et al., 1999 ; Togneri et al., 2001). Second, the AIMM approximates the Gaussian mixture with a single Gaussian density. If these assumptions break down, the AIMM-EKF may diverge. In this study, because of these drawbacks of the AIMM-EKF, an unscented Kalman filter (UKF) (Julier and Uhlmann, 1997 ; Julier et al., 1995 ; 2000 ; Ristic and Arulampalam, 2003), replacing the EKF, is used for the curvilinear model. The algorithm itself uses the same AIMM logic, but the model-matched EKF is replaced by the model-matched UKF.

The objective of this paper is to design an UKF for curvilinear motions in an IMM algorithm to detect and avoid other AGVs for the autonomous navigation of an AGV in an automated port.

The contributions of this paper are as follows : First, in an automated container terminal, the IMM algorithm is provided as a navigation algorithm for AGVs in navigating autonomously. Second, two kinematic models for the possible navigation patterns of AGVs are derived : A constant velocity model for linear motions and a constant-speed turn model for curvilinear motions are discussed. Third, for the constant- speed turn model, an UKF is used because of the drawbacks of the EKF. Fourth, the suggested algorithm reduces the root mean squares error in the case of rectilinear motions and detects the occurrence of maneuvering quickly in the case of turning motions.

This paper is organized as follows : In Section 2, we provide the various navigation patterns of AGVs. A stochastic hybrid system is formulated, and two kinematic models are discussed. In Section 3, we compare an UKF with an EKF for a constant-speed turn model in an IMM algorithm. In Section 4, we evaluate the performance of these filters using Monte Carlo simulation under the various patterns. Section 5 concludes the paper.

2. Problem Formulation

In this section, after analyzing the navigation patterns of an AGV in a terminal, a stochastic hybrid system in the form of an IMM algorithm for detecting other AGVs using sensors (radar, lidar, laser scanner, sonar, vision, etc.) is formulated. Also, two kinematic models representing the analyzed navigation patterns are introduced.

2.1 Navigation patterns

Figure 2 depicts the various navigation patterns of an AGV (Lee et al., 2003) : straight line and curve, cut-in/out, and u-turn. All of these patterns can be represented by a combination of a constant-velocity rectilinear motion, a constant-acceleration rectilinear motion, a constant angular velocity curvilinear motion, and a constant angular acceleration curvilinear motion. As kinematic models for describing these motions, two stochastic models will be investigated : one for rectilinear motion and the other for curvilinear motion. These typical navigation patterns are described briefly as follows :

(i) Straight line and curve: In this situation, the AGV detects a preceding AGV that follows straight lines and curves on a curved road (Lauffenburger et al., 2003; Rajamani et al., 2003).

(ii) Cut-in/out: The cut-in/out indicates the situation in which a maneuvering AGV cuts in (or out) to (or from) the lane while the AGV is tracking other AGV. In this situation, the detection of up to three surrounding AGVs is assumed: one in front, one to the left, and one to the right. In this case, the target AGV changes its motion from a rectilinear motion to a curvilinear motion and then back to a rectilinear motion.

(iii) U-turn: This situation occurs when the target AGV changes its driving direction by 180°. The u-turn consists of three routes as follows: The target AGV moves rectilinearly, undergoes a uniform circular turning of up to 180° with a constant yaw rate, and then converts to a rectilinear motion in the opposite direction.

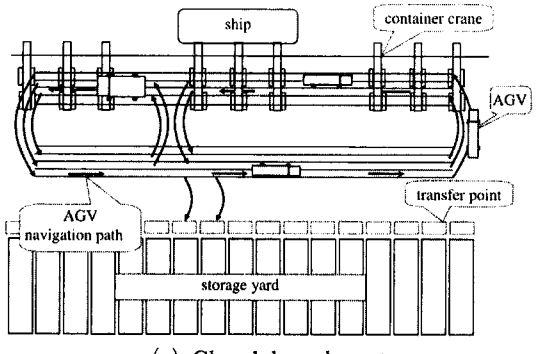

(a) Closed-loop layout

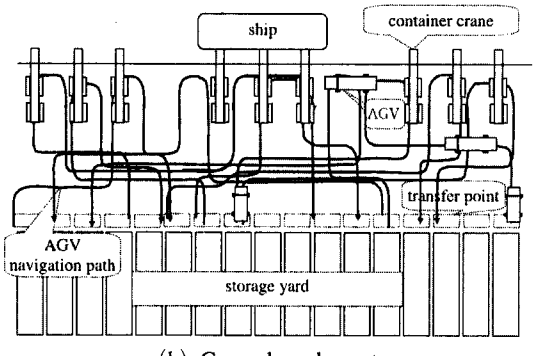

(b) Cross-lane layout

Fig. 2 Various navigation patterns of AGVs

It will be shown in the sequel that a constant velocity model will capture both constant velocity and acceleration rectilinear motions without and with an additional noise term, respectively. On the other hand, a constant-speed turn model will cover both constant angular velocity and angular acceleration curvilinear motions without and with a noise term, respectively.

2.2 Stochastic hybrid system

Following the work of Li and Bar-Shalom (1993), a stochastic hybrid system with additive noise is considered as follows:

$$x(k)=f[k-1, x(k-1), m(k)] +g[k-1, x(k-1), \nu[k-1, m(k)], m(k)] \quad (1)$$

with noisy measurements

$$z(k)=h[k, x(k), m(k)]+w[k, m(k)] \quad (2)$$

where $x(k)\in\Re^{n_x}$ is the state vector including the position, velocity, and yaw rate of the AGV at discrete time k. $m(k)$ is the scalar-valued modal state (navigation mode index) at instant k, which is a homogeneous Markov chain with probabilities of transition given by

$$P\{m_j(k+1)\,|\,m_i(k)\}=\pi_{ij},\ \forall m_i,\ m_j\in\mathrm{M} \quad (3)$$

where $P\{\cdot\}$ denotes the probability and M is the set of modal states, i.e., constant velocity, constant acceleration, constant angular rate turning with a constant radius of curvature, etc. The considered system is hybrid since the discrete event $m(k)$ appears in the system. In the autonomous navigation of AGV, $m(k)$ denotes the navigation mode of the preceding AGV, in effect during the sampling period ending at k, i.e., the time period $(k_{k-1}, t_k]$. The event for which a mode m_j is in effect at time k is denoted as

$$m_j(k)\triangleq\{m(k)=m_j\} \quad (4)$$

$z(k)\in\Re^{n_z}$ is the vector-valued noisy measurement from the sensor at time k, which is mode-dependent. $\nu[k-1, m(k)]\in\Re^{n_v}$ is the mode-dependent process noise sequence with mean $\bar{\nu}[k-1, m(k)]$ and covariance $Q[k-1, m(k)]$. $w[k, m(k)]\in\Re^{n_z}$ is the mode-dependent measurement noise sequence with mean $\bar{w}[k, m(k)]$

and covariance $R[k, m(k)]$. Finally f, g, and h are nonlinear vector-valued functions.

2.3 Two kinematic models

The concept of using noise-driven kinematic models comes from the fact that noises with different levels of variance can represent different motions. A model with high variance noise can capture maneuvering motions, while a model with low variance noise represents uniform motions. The multiple-models approach assumes that a model can immediately capture the complex system behavior better than others.

Two kinematic models for rectilinear and curvilinear motions are now derived : First, assuming that accelerations in the steady state are quite small (abrupt motions like a sudden stop or a collision are not covered), linear accelerations or decelerations can be reasonably well covered by process noises with the constant velocity model. That is, the constant velocity model plus a zero-mean noise with an appropriate covariance representing the magnitude of acceleration can handle uniform motions on the road. In discrete-time, the constant velocity model with noise is given by

$$x(k)=\begin{bmatrix}1 & T & 0 & 0\\ 0 & 1 & 0 & 0\\ 0 & 0 & 1 & T\\ 0 & 0 & 0 & 1\end{bmatrix}x(k-1)+\begin{bmatrix}1/2T^2 & 0\\ T & 0\\ 0 & 1/2T^2\\ 0 & T\end{bmatrix}\nu(k-1) \quad (5)$$

where T is the sampling time (0.01 sec), $x(k)$ is the state vector including the position and velocity of the preceding vehicle in the longitudinal (ξ) and lateral (η) directions at discrete time k, i.e.,

$$x(k)=[\xi(k)\ \dot{\xi}(k)\ \eta(k)\ \dot{\eta}(k)]' \quad (6)$$

with ξ and η denoting the orthogonal coordinates of the horizontal plane; and ν is a zero-mean Gaussian white noise representing the accelerations with an appropriate covariance Q. If $\nu(k)$ is the acceleration increment during the kth sampling period, the velocity during this period is calculated by $\nu(k)\,T$, and the position is altered by $\nu(k)\,T^2/2$.

Second, a discrete-time model for turning is derived from a continuous-time model for the coordinated turn motion (Bar-Shalom et al., 2001). A constant speed turn is a turn with a constant yaw rate along a road of constant radius of curvature. However, the curvatures of actual roads are not constant. Hence, a fairly small noise is added to a constant-speed turn model for the purpose of capturing the variation of the road curvature. The noise in the model represents the modeling error, such as the presence of angular acceleration and a non-constant radius of curvature. For a vehicle turning with a constant angular rate and moving with constant speed (the magnitude of the velocity vector is constant), the kinematic equations in the (ξ, η) plane are

$$\ddot{\xi}(t)=-\omega\dot{\eta}(t),\ \ddot{\eta}(t)=\omega\dot{\xi}(t) \quad (7)$$

where $\ddot{\xi}(t)$ is the normal (longitudinal) acceleration and $\ddot{\eta}(t)$ denotes the tangential acceleration, and ω is the constant yaw rate ($\omega>0$ implies a counterclockwise turn). The tangential component of the acceleration is equal to the rate of change of the speed, i.e., $\ddot{\eta}(t)=d\dot{\eta}(t)/dt=d(\omega\xi(t))/dt$, and the normal component is defined as the square of the speed in the tangential direction divided by the radius of the curvature of the path, i.e., $\ddot{\xi}(t)=-\dot{\eta}^2(t)/\xi(t)=-\omega^2\xi^2(t)/\xi(t)$ where $\dot{\eta}(t)=\omega\xi(t)$. The state space representation of Eq. (7) with the state vector defined by $x(t)=[\xi(t)\ \dot{\xi}(t)\ \eta(t)\ \dot{\eta}(t)]'$ becomes

$$\dot{x}(t)=Ax(t) \quad (8)$$

where

$$A=\begin{bmatrix}0 & 1 & 0 & 0\\ 0 & 0 & 0 & -\omega\\ 0 & 0 & 0 & 1\\ 0 & \omega & 0 & 0\end{bmatrix}$$

The state transient matrix of the system, Eq. (8) is given by

$$e^{At}=\begin{bmatrix}1 & \dfrac{\sin\omega t}{\omega} & 0 & \dfrac{1-\cos\omega t}{\omega}\\ 0 & \cos\omega t & 0 & -\sin\omega t\\ 0 & \dfrac{1-\cos\omega t}{\omega} & 1 & \dfrac{-\sin\omega t}{\omega}\\ 0 & \sin\omega t & 0 & \cos\omega t\end{bmatrix} \quad (9)$$

It is remarked that if the angular rate ω in Eq. (7) is time-varying, Eq. (9) would be no longer true. In the sequel, following the approach in (Bar-Shalom et al., 2001), a "nearly" constant speed turn model in a discrete-time domain is introduced. In this approach, the model itself is motivated from Eq. (9), but the angular rate is allowed to vary.

A new state vector by augmenting the angular rate $\omega(k)$ to the state vector of Eq. (7) is defined as follows:

$$x^a(k)=[\xi(k)\ \ \dot{\xi}(k)\ \ \eta(k)\ \ \dot{\eta}(k)\ \ \omega(k)]' \quad (10)$$

where superscript a denotes the augmented value. Then, the nearly constant speed turn model is defined as follows (Bar-Shalom et al., 2001):

$$x^a(k)=\begin{bmatrix} 1 & \frac{\sin\omega(k-1)T}{\omega(k-1)} & 0 & -\frac{1-\cos\omega(k-1)T}{\omega(k-1)} & 0 \\ 0 & \cos\omega(k-1)T & 0 & -\sin\omega(k-1)T & 0 \\ 0 & \frac{1-\cos\omega(k-1)T}{\omega(k-1)} & 1 & \frac{\sin\omega(k-1)T}{\omega(k-1)} & 0 \\ 0 & \sin\omega(k-1)T & 0 & \cos\omega(k-1)T & 0 \\ 0 & 0 & 0 & 0 & 1 \end{bmatrix} x^a(k-1) + \begin{bmatrix} \frac{T^2}{2} & 0 & 0 \\ T & 0 & 0 \\ 0 & \frac{T^2}{2} & 0 \\ 0 & T & 0 \\ 0 & 0 & T \end{bmatrix} \nu^a(k-1) \quad (11)$$

Evidently, both Eq. (5) and Eq. (11) are special forms of Eq. (1). In addition, it is reasonable to assume that the transition between the navigation modes of an AGV has the Markovian probability governed by Eq. (3). Consequently, the kinematic behaviors of an AGV can be suitably described in the framework of the stochastic hybrid systems.

3. Proposed Unscented Kalman Filter for Turning Motions

The concept (structure) of an IMM algorithm is referred to in (Bar-Shalom et al., 2001) and (Li and Bar-Shalom, 1993). In this study two models in the IMM algorithm are used: one for rectilinear motion and the other for curvilinear motion. The tracking procedure of the AGV in a rectilinear motion using Eq. (5) is carried out by the standard Kalman filter, which is not discussed in this paper. However, for tracking curvilinear motions, which requires the estimation of ω with a new augmented model Eq. (8) in Sec. 2, an UKF is used.

3.1 The EKF for the constant-speed turn model

Since the model in Eq. (11) is nonlinear, the estimation of the state, Eq. (10) will be performed via the EKF. The nearly constant-speed turn model of Eq. (11) can be rewritten as follows:

$$x^a(k)=f^a[x^a(k-1),\ \omega(k-1)] + G(k-1)\,\nu^a(k-1) \quad (12)$$

where the function $f^a(\cdot)$ is known and remains unchanged during the estimation procedure. The noise transition matrix $G(k-1)$ is the same form as that given in Eq. (11). To obtain the predicted state $\hat{x}^a(k|k-1)$, the nonlinear function in Eq. (12) is expanded in Taylor series around the latest estimate $\hat{x}^a(k-1|k-1)$ with terms up to first order, to yield the first-order EKF. The vector Taylor series expansion of Eq. (12) up to first order is

$$x^a(k)=f^a[\hat{x}^a(k-1|k-1),\ \omega(k-1)] + f^a_{x^a}(k-1)[x^a(k-1)-\hat{x}^a(k-1|k-1)] + \text{HOT} + G(k-1)\,\nu^a(k-1) \quad (13)$$

where HOT represents the higher-order terms and

$$f^a_{x^a}(k-1)=[\nabla_{x^a} f^a(x^a,\omega)']'\big|_{x^a=\hat{x}^a(k-1|k-1)} = \begin{bmatrix} 1 & \frac{\sin\hat{\omega}(k-1)T}{\hat{\omega}(k-1)} & 0 & -\frac{1-\cos\hat{\omega}(k-1)T}{\hat{\omega}(k-1)} & f_{\omega,1}(k-1) \\ 0 & \cos\hat{\omega}(k-1)T & 0 & -\sin\hat{\omega}(k-1)T & f_{\omega,2}(k-1) \\ 0 & \frac{1-\cos\hat{\omega}(k-1)T}{\hat{\omega}(k-1)} & 1 & \frac{\sin\hat{\omega}(k-1)T}{\hat{\omega}(k-1)} & f_{\omega,3}(k-1) \\ 0 & \sin\omega(k-1)T & 0 & \cos\hat{\omega}(k-1)T & f_{\omega,4}(k-1) \\ 0 & 0 & 0 & 0 & 1 \end{bmatrix} \quad (14)$$

is the Jacobian of the vector f evaluated at the latest estimate of the state. The partial derivatives with respect to ω are given by

Table 1 Summary of the EKF in an IMM algorithm (one cycle)

	Filtering
predicted estimate :	$\hat{x}^a(k\|k-1)=f^a(\hat{x}_0{}^a(k-1\|k),\ \omega(k-1))$
predicted covariance :	$P^a(k\|k-1)=f^a_{x^a}(k-1)\,P^a_0(k-1\|k-1)\,f'^a_{x^a}(k-1)+G(k-1)\,Q^a(k-1)\,G'(k-1)$
measurement residual :	$v(k)\triangleq z(k)-H\hat{x}^a(k\|k-1)$
residual covariance :	$S(k)=HP^a(k\|k-1)\,H'+R(k)$
filter gain :	$K^a(k)=P^a(k\|k-1)\,H'S^{-1}(k)$
updated estimate :	$\hat{x}^a(k\|k)=\hat{x}^a(k\|k-1)+K^a(k)\,v(k)$
updated covariance :	$P^a(k\|k)=P^a(k\|k-1)-K^a(K)\,S(k)\,(K^a(k))'$
likelihood function :	$\Lambda=N[v\,;\,0,\,S]=\lvert 2\pi S\rvert^{-2/2}e^{-\frac{1}{v}S-1v}$
mode probability :	$\mu=\frac{\mu^-\Lambda}{\sum_i\mu_i^-\Lambda_i}$

$$
\begin{aligned}
f_{\omega,1}&=\frac{T\hat{\xi}(k-1|k-1)\cos\hat{\omega}(k-1)T}{\hat{\omega}(k-1)}-\frac{\hat{\xi}(k-1|k-1)\sin\hat{\omega}(k-1)T}{\hat{\omega}(k-1)^2}\\
&\quad-\frac{T\hat{\eta}(k-1|k-1)\sin\hat{\omega}(k-1)T}{\hat{\omega}(k-1)}-\frac{\hat{\eta}(k-1|k-1)(-1+\cos\hat{\omega}(k-1)T)}{\hat{\omega}(k-1)^2}\\
f_{\omega,2}&=-T\hat{\xi}(k-1|k-1)\sin\hat{\omega}(k-1)-T\hat{\eta}(k-1|k-1)\cos\hat{\omega}(k-1)\\
f_{\omega,3}&=\frac{T\hat{\xi}(k-1|k-1)\sin\hat{\omega}(k-1)T}{\hat{\omega}(k-1)}-\frac{\hat{\xi}(k-1|k-1)(1-\cos\hat{\omega}(k-1)T)}{\hat{\omega}(k-1)^2}\\
&\quad+\frac{T\hat{\eta}(k-1|k-1)\cos\hat{\omega}(k-1)T}{\hat{\omega}(k-1)}-\frac{\hat{\eta}(k-1|k-1)\sin\hat{\omega}(k-1)T}{\hat{\omega}(k-1)^2}\\
f_{\omega,4}&=T\hat{\xi}(k-1|k-1)\cos\hat{\omega}(k-1)-T\hat{\eta}(k-1|k-1)\sin\hat{\omega}(k-1)
\end{aligned}
\tag{15}
$$

Based on the above expansion, the state prediction and state prediction covariance in the EKF are

$$\hat{x}^a(k|k-1)=f^a[\hat{x}^a(k-1|k-1),\ \omega(k-1)] \tag{16}$$

$$
\begin{aligned}
P^a(k|k-1)&=f^a_{x^a}(k-1)\,P^a(k-1|k-1)\,f'^a_{x^a}(x-1)\\
&\quad+G(k-1)\,Q^a(k-1)\,G'(k-1)
\end{aligned}
\tag{17}
$$

where Q^a is the covariance of the process noise in Eq. (12). The details of the EKF in an IMM algorithm during one cycle are given in Table 1.

Remark 1: When target dynamics is described by multiple-switching models, the posterior density of the state vector is a mixture density (Bar-Shalom et al., 2001). The EKF approximates the mixture components with the Gaussian probability density function. The goal of the IMM algorithm is to merge all mixture components into a single Gaussian distribution in such a way that the first and the second moment are matched. The main point is that for each dynamic model a separate filter is used. In this study, we use two Kalman-based filters for two stochastic models : one for rectilinear motion and the other for curvilinear motion. The results of these two model-matched filters are mixed before filtering. The outputs of the model-matched Kalman based filters at time t_k include : the state estimate $\hat{x}^a(k|k)$, covariance $P^a(k|k)$ and the model probability $\mu(k)$. The overall output of the IMM algorithm is then calculated using the Gaussian mixture equations. The drawbacks of the IMM algorithm using an EKF are as follows : First, the EKF approximates a non-Gaussian density by a Gaussian density (Katsikas et al., 1995 ; Tam et al., 1999 ; Togneri et al., 2001). Second, the IMM algorithm approximates the Gaussian mixture by a single Gaussian density. If these assumptions break down, the IMM algorithm using an EKF may diverge.

3.2 The UKF for the constant-speed turn model

Because of the well-known drawbacks of the EKF, the UKF for the constant-speed turn model is used (Julier et al., 1995 ; Julier and Uhlmann, 1997 ; Julier et al., 2000 ; Ristic and Arulampalam, 2003).

Similarly to the EKF, the UKF is a recursive minimum mean square error estimator. But unlike the EKF, which only uses the first-order terms in the Taylor series expansion of the non-linear measurement equation, the UKF uses the true measurement model and approximates the distribution of the state vector. This state distribution is still represented by a Gaussian density, but it is

specified with a set of deterministically chosen sample (or sigma) points. The sample points completely capture the true mean and covariance of the Gaussian random vector. When propagated though any non-linear system, the sample points capture the posterior mean and covariance accurately to the second order. The main building block of the UKF is the unscented transform, described below.

The unscented transform is a method for calculating the statistics of a random vector which undergoes a non-linear transformation. Let $x\in\Re^{n_x}$ be a random vector, $p:\Re^{n_x}\rightarrow\Re^{n_y}$ a non-linear transformation and $y=p(x)$. Assume that the mean and the covariance of x are $\bar{x}$ and P_x, respectively. The procedure for calculating the first two moments of y using the unscented transform is as follows (Julier et al., 2000) :

(1) Compute $(2n_x+1)$ sigma points χ_i and their weights W_i :

$$\begin{aligned}
&\chi_0=\bar{x}, && W_0=\frac{\kappa}{n_x+\kappa},\ i=0,\\
&\chi_i=\bar{x}+(\sqrt{(n_x+\kappa)P_x})_i, && W_i=\frac{1}{2(n_x+\kappa)},\ i=1,\cdots,n_x\\
&\chi_i=\bar{x}-(\sqrt{(n_x+\kappa)P_x}) && W_i=\frac{1}{2(n_x+\kappa)},\ i=n_x+1,2n_x
\end{aligned}\tag{18}$$

where κ is a scaling parameter for fine tuning the higher order moments of the approximation and $(\sqrt{(n_x+\kappa)P_x})_i$ is the ith row or column of the matrix square root of $(n_x+\kappa)P_x$.

(2) Propagate each sigma point through the non-linear function

$$\zeta_i=p(\chi_i)\quad(i=0,\cdots,2n_x)\tag{19}$$

(3) Calculate the mean and covariance of y as follows :

$$\begin{aligned}
\bar{y}&=\sum_{i=0}^{2n_x}W_i\zeta_i\\
P_y&=\sum_{i=0}^{2n_x}W_i(\zeta_i-\bar{y})(\zeta_i-\bar{y})'
\end{aligned}\tag{20}$$

Next, the UKF for the constant-speed turn model is derived as follows :

(1) Using Eq. (18), compute the sigma points $\chi_i(k-1|k-1)$ and the weights $W_i(i=0,\cdots,2n)$ corresponding to $\hat{x}^a(k-1|k-1)$ and $P^a(k-1|k+1)$.

(2) Predict the sigma points using the state equation, Eq. (12) as follows :

$$\chi_i(k|k-1)=f^a[\chi_i(k-1|k-1),\ \omega(k-1)]\tag{21}$$

(3) Compute the predicted mean and covariance of the state variable $\hat{x}^a(k|k-1)$ and $P^a(k|k-1)$, using the prediction sigma points $\chi_i(k|k-)\in\Re^n$ and their weights $W_i(i=0,\cdots,2n)$.

$$\begin{aligned}
\hat{x}^a(k|k-1)&=\sum_{i=0}^{2n}W_i\chi_i(k|k-1)\\
P_a(k|k-1)&=Q^a+\sum_{i=0}^{2n}W_i[\chi_i(k|k-1)-x^a(k|k-1)]\\
&\quad[\chi_i(k|k-1)-x^a(k|k-1)]'
\end{aligned}\tag{22}$$

(4) Predict the measurement sigma points $\Im_i(k|k-1)$ using Eq. (2),

$$\Im_i(k|k-1)=h[\chi_i(k|k-1),\ \omega(k)]\tag{23}$$

(5) Predict the measurement and covariances

$$\begin{aligned}
\hat{z}^a(k|k-1)&=\sum_{i=0}^{2n}W_i\Im_i(k|k-1)\\
P_{zz}^a&=R(k)+\sum_{i=0}^{2n}W_i[\Im_i(k|k-1)-\hat{z}^a(k|k-1)]\\
&\quad[\Im_i(k|k-1)-\hat{z}^a(k|k-1)]'\\
P_{xz}^a&=\sum_{i=0}^{2n}W_i[\chi_i(k|k-1)-\hat{x}^a(k|k-1)]\\
&\quad[\Im_i(k|k-1)-\hat{z}^a(k|k-1)]'
\end{aligned}\tag{24}$$

where P_{zz}^a and P_{xz}^a are, respectively, the covariance matrix of the measurement and the cross-covariance of the measurement and state variable.

(6) Compute the filter gain as

$$K^a(k)=P_{xz}^a(P_{zz}^a)^{-1}\tag{25}$$

Update the UKF with measurement $z(k)$:

$$\begin{aligned}
\hat{x}^a(k|k)&=\hat{x}^a(k|k-1)\\
&\quad+K^a(k)[z(k)-\hat{z}^a(k|k-1)]
\end{aligned}\tag{26}$$

$$P^a(k|k)=P^a(k|k-1)-K^a(k)P_{zz}^aK'^a(k)\tag{27}$$

Note that the UKF requires the computation of a matrix square root in Eq. (18), which can be performed using the Cholesky factorization.

Remark 2: In the unscented transformation, on which the UKF is based, a set of weighted sigma points are deterministically chosen so that

certain properties of these points match those of the prior distribution. Each point is then propagated through a non-linear function and the properties of the transformed set are calculated. With this set of points, the unscented transform guarantees the same performance as the truncated second order Gaussian filter, with the same order of calculations as an EKF but without the need to calculate Jacobians.

4. Simulations Results

As described in this section, we considered a state estimation problem of an AGV in two dimensions. Simulations were executed to compare the performance of both IMM algorithms using the EKF and the UKF, respectively, for curvilinear motion. The performance of the two algorithms was compared with the use of Monte Carlo simulations. The maneuvering AGV trajectories were generated using the various patterns mentioned in Sec 2.1. Two kinematic models were used to track the maneuvering AGV : A constant-velocity model for rectilinear motion and a constant- speed turn model for curvilinear motion. We then compare the performance of two different IMM algorithms with these two models.

4.1 The navigation scenario

It was assumed that the AGV navigates rectilinearly in the beginning. The target initial positions and velocities were differently set for each scenario. The single-target track of the maneuvering AGV was also assumed to have been previously initialized and that track maintenance was the goal of the IMM algorithms. The results for 3 selected scenarios are presented, according to the cross-lane layout, in Fig. 2.

(i) Scenario for straight line and curve : The target initial positions and velocities were (x_0= 10 m, y_0=10 m, $\dot{x}_0$=0 m/s, $\dot{y}_0$=6 m/s, ω=0°/s). Its trajectory was a constant velocity between 0 s and 500 s with a speed of 6 m/s ; a turn with a constant yaw rate of $\omega=-3°$/s between 500 s and 848 s ; a constant velocity between 848 s and 1182 s ; a turn with a constant yaw rate of ω=3°/s between 1182 s and 1531 s ; a constant velocity between 1531 s and 3049 s.

(ii) Cut-in/out scenario : The target initial positions and velocities were (x_0=10 m, y_0=10 m, $\dot{x}_0$=0 m/s, $\dot{y}_0$=6 m/s, ω=0°/s). Its trajectory was a straight line between 0 s and 333 s with a speed of 6 m/s ; a turn with a constant yaw rate of $\omega=-1.2°$/s between 333 s and 376 s ; a straight line between 376 s and 476 s with a speed of 6 m/s ; a turn between 476 s and 520 s with a yaw rate of ω=1.2°/s ; a straight line between 520 s and 687 s with a speed of 6 m/s ; a turn with a constant yaw rate of ω=1.2°/s between 687 s and 730 s ; a straight line between 730 s and 830 s with a speed of 6 m/s ; a turn between 830 s and 874 s with a yaw rate of $\omega=-1.2°$/s, and a straight line from scan 874 s to 1200 s.

(iii) U-turn scenario : The target initial positions and velocities were (x_0=10 m, y_0=10 m, $\dot{x}_0$=0 m/s, $\dot{y}$=6 m/s, ω=0°/s). This scenario included a non-maneuvering navigation mode during scans from 0 s to 333 s with a speed of 6 m/s, a 180°-turn, lasting from scan 333 s to 411 s with a yaw rate of $\omega=-4°$/s, and a non-maneuvering navigation mode from scan 411 s to 747 s.

4.2 Parameters used in the design

The parameters used in the design are listed here. Subscripts "CV" and "CST" stand for "constant velocity" and "constant speed turn," respectively. The initial yaw rate of each navigation scenario was $\omega(0)$=3°/s, 1.2°/s, and 4°/s, respectively. The error covariances of the initial state and covariances of process noise were as follows :

$$P^{CV}(0)=\text{diag}\{0.5\ 0.1\ 0.5\ 0.1\},\ Q^{CV}=0.01\mathrm{I}$$

$$P^{CST}(0)=\text{diag}\{0.5\ 0.1\ 0.5\ 0.1\ \sigma_\omega^2\},\ Q^{CST}=\mathrm{I}$$

where $\sigma_\omega=(0.1)°$/s. The measurement noise covariance matrix was calculated as σ_ξ=0.05 m and σ_η=0.005 m, respectively.

The transition probabilities for the IMM algorithms using the EKF and the UKF, respectively, were represented in the Markov chain transition matrix

$$\pi_{ij}^{EKF}=\pi_{ij}^{UKF}=\begin{bmatrix}0.9 & 0.1\\ 0.1 & 0.9\end{bmatrix}\pi_{ij}$$

The initial mode probability vectors μ were chosen as follows:

$$\mu^{EKF}=\mu^{UKF}=\begin{bmatrix}0.5\\ 0.5\end{bmatrix}$$

4.3 Performance evaluation and analysis

The RMSE of each state component was chosen as the measure of performance. The performance of the IMM algorithm with an EKF and that of the IMM algorithm with an UKF are shown in Figs. 3~8, where the RMSE in the position and the velocity are plotted. The results presented here are based on 100 Monte Carlo runs. First of all, it is evident that the suggested algorithm has almost equal position and velocity estimation accuracy for all scenarios. The position RMSE of the IMM with an UKF is evidently superior to that of the IMM with an EKF. This is because, unlikely EKF, UKF does not approximate nonlinear functions but directly propagates mean and covariance through the nonlinear system equation. In addition, the IMM algorithm with an UKF is characterized by lower-peak dynamic errors and a shorter response time. These conclusions were confirmed by the RMSE plot presented in Figs. 3~8, respectively.

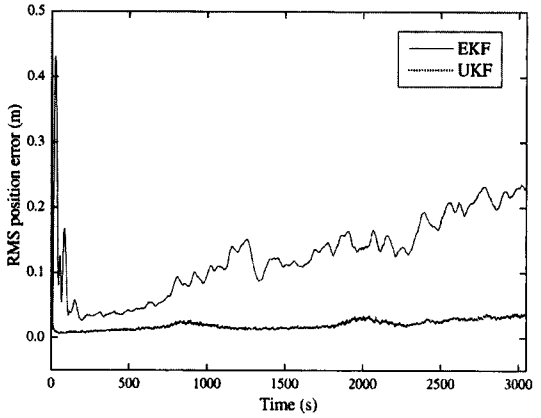

Fig. 3 Comparison of the position errors in the case of straight lines and curves

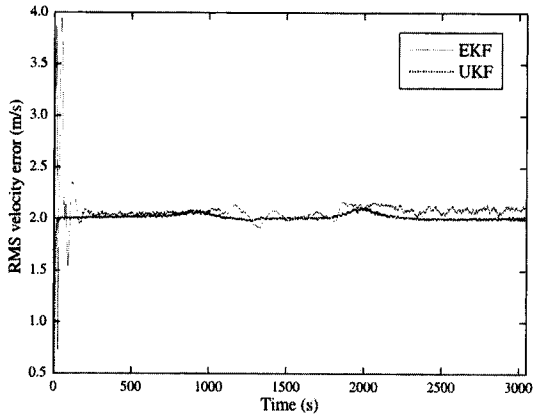

Fig. 4 Comparison of the velocity errors in the case of straight lines and curves

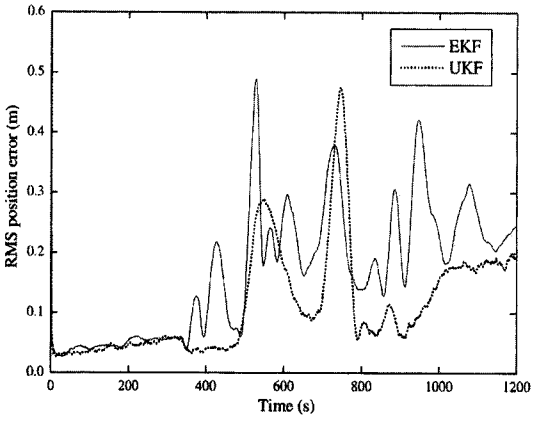

Fig. 5 Comparison of the position errors in the case of cut-in/out

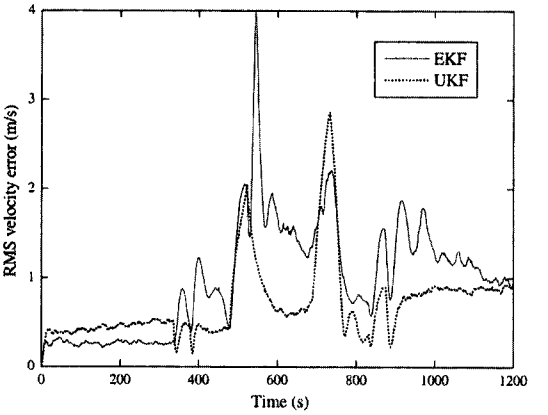

Fig. 6 Comparison of the velocity errors in the case of cut-in/out

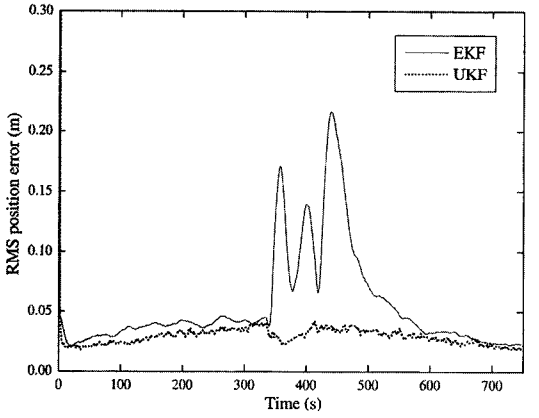

Fig. 7 Comparison of the position errors in the case of u-turn

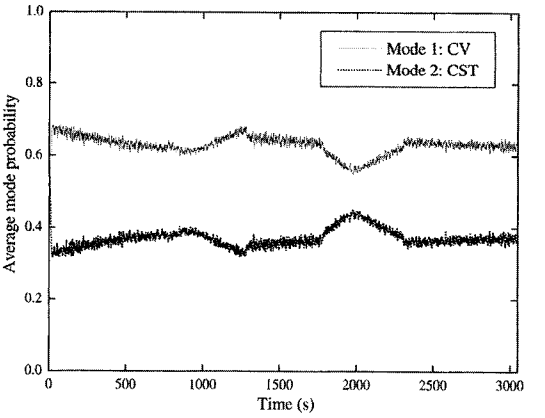

Fig. 10 Average mode probability of an UKF in the case of straight lines and curves

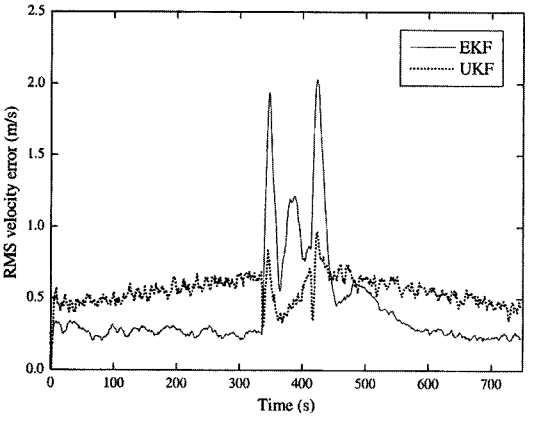

Fig. 8 Comparison of the velocity errors in the case of u-turn

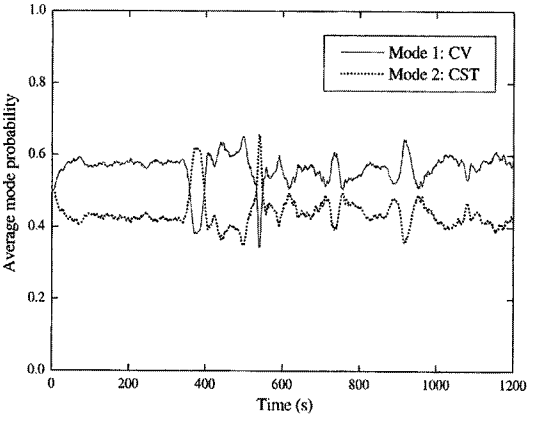

Fig. 11 Average mode probability of an EKF in the case of cut-in/out

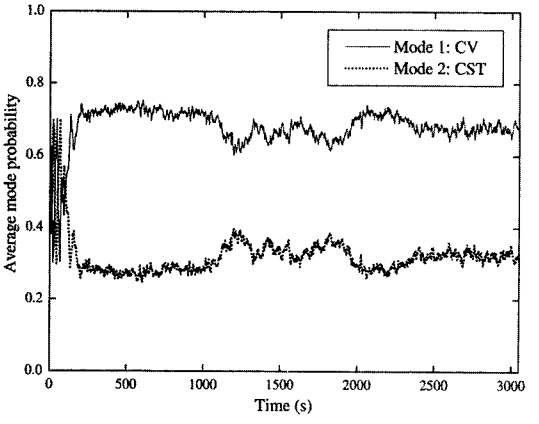

Fig. 9 Average mode probability of an EKF in the case of straight lines and curves

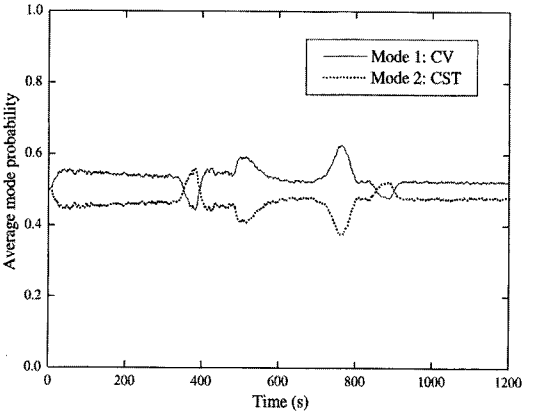

Fig. 12 Average mode probability of an UKF in the case of cut-in/out

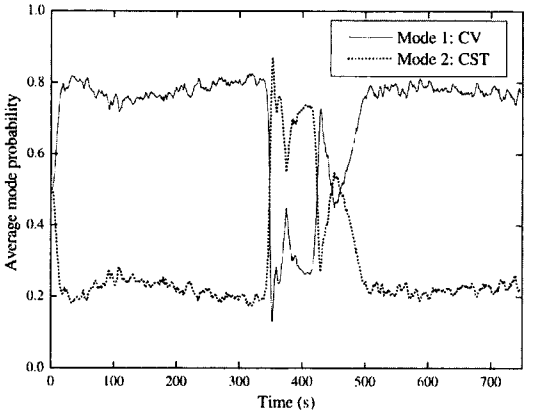

Fig. 13 Average mode probability of an EKF in the case of u-turn

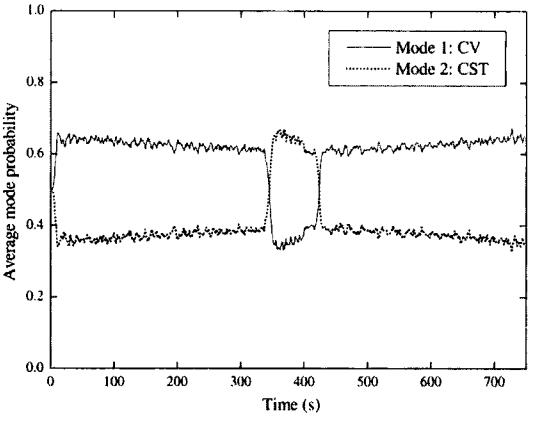

Fig. 14 Average mode probability of an UKF in the case of u-turn

Figures. 9~14 show the average mode probability of the IMM algorithm with an EKF and that of the IMM algorithm with an UKF. As can be seen from these Figures, the average mode probability of IMM algorithms represents rapid detection for each driving mode. This is due to the mode adaptation of the suggested IMM algorithms.

5. Conclusions

In this paper, a tracking algorithm for AGVs operated in automated container terminal was designed. As models to detect other AGVs, two kinematic models were derived : The constant-velocity model for linear motion and the constant-speed turn model for curvilinear motion. For the constant-speed turn model, an unscented Kalman filter was used because of the drawbacks of the extended Kalman filter in nonlinear systems. The suggested algorithm reduced the root mean squares error for linear motions, and it could rapidly detect possible turning motions.

Acknowledgment

This work was supported by the Ministry of Science and Technology of Korea under a program of the National Research Laboratory, grant number NRL M1-0302-00-0039-03-J00-00-023-10.

References

Adam, A., Rivlin, E. and Rotstein, H., 1999, "Fusion of Fixation and Odometry for Vehicle Navigation," *IEEE Transactions on Systems, Man, and Cybernetics-Part A : Systems and Humans*, Vol. 29, No. 6, pp. 593~603.

Bar-Shalom, Y., Li, X. and Kirubarajan, T., 2001, *Estimation with Applications to Tracking and Navigation*, John Wiley & Sons, INC, New York, pp. 421~490.

Ding, Z., Leung, H., Chan, K. and Zhu, Z., 2001, "Model-Set Adaptation Using a Fuzzy Kalman Filter," *Mathematical and Computer Modelling*, Vol. 34, No. 7-8, pp. 799~812.

Dufour, F. and Mariton, M., 1992, Passive Sensor Data Fusion and Maneuvering Target Tracking, *In Multitarget-Multisensor Tracking : Applications and Advances* (Edited by Bar-Shalom, Y.), Artech House, Norwood, MA, Chapter 3, pp. 65~92.

Efe, M. and Atherton, D. P., 1996, "Maneuvering Target Tracking Using Adaptive Turn Rate Models in the Interacting Multiple Model Algorithm," *Proceedings of the 35th Conference on Decision and Control*, Kobe, Japan, 11-13 December, pp. 3151~3156.

Efe, M., Bather, J. A. and Atherton, D. P., 1999, "An Adaptive Kalman Filter with Sequential Rescaling of Process Noise," *Proceedings of the*

American Control Conference, San Diego, California, USA, 2-4 June, pp. 3913~3917.

Farina, A., 1999, "Target Tracking with Bearings-Only Measurements," *Signal Processing*, Vol. 78, No. 1, pp. 61~78.

Helferty, J. P., 1996, "Improved Tracking of Maneuvering Targets: The Use of Turn-Rate Distributions for Acceleration Modeling," *IEEE Transactions on Aerospace and Electronic Systems*, Vol. 32, No. 4, pp. 1355~1361.

Houles, A. and Bar-Shalom, Y., 1989, "Multisensor Tracking of a Maneuvering Target in Clutter," *IEEE Transactions on Aerospace and Electronic Systems*, Vol. 25, No. 2, pp. 176~189.

Ioannou, P. A., Jula, H. and Dougherty, E. Jr., 2001, "Advanced Material Handling: Automated Guided Vehicles in Agile Ports," *Technical Report*, Center for Advanced Transportation Technologies, University of Southern California.

Jilkov, V. P., Angelova, D. S. and Semerdjiev, TZ. A., 1999, "Design and Comparison of Mode-Set Adaptive IMM Algorithms for Maneuvering Target Tracking," *IEEE Transactions on Aerospace and Electronic Systems*, Vol. 35, No. 1, pp. 343~350.

Jin, T. S., Lee, B. K. and Lee, J. M., 2003, "AGV Navigation Using a Space and Time Sensor Fusion of an Active Camera," *International Journal of Navigation and Port Research*, Vol. 27, No. 3, pp. 273~282.

Julier, S. J. and Uhlmann, J. K., 1997, "A New Extension of the Kalman Filter to Nonlinear Systems," *Proceedings of Aerosense : SPIE's 11th International Symposium on Aerospace/Defense Sensing, Simulation and Controls*, Orlando, FL, USA, 21-25 April, Vol. 3068, pp. 182~193.

Julier, S. J., Uhlmann, J. K. and Durrant-Whyte, H. F., 2000, "A New Method for the Nonlinear Transformation of Means and Covariances in Filters and Estimators," *IEEE Transactions on Automatic Control*, Vol. 45, No. 3, pp. 477~482.

Julier, S. J., Uhlmann, J. K. and Durrant-Whyte, H. F., 1995, "A New Approach for Filtering Nonlinear Systems," *Proceedings of the American Control Conference*, Seattle, Washington, USA, 21-23 June, Vol. 3, pp. 1628~1632.

Katsikas, S. K., Leros, A. K. and Lainiotis, D. G., 1995, "Underwater Tracking of a Maneuvering Target Using Time Delay Measurements," *Signal Processing*, Vol. 41, No. 1, pp. 17~29.

Kim, Y. S. and Hong, K. S., 2004, "An IMM Algorithm for Tracking Maneuvering Vehicles in an Adaptive Cruise Control Environment," *International Journal of Control, Automation, and Systems*, Vol. 2, No. 3, pp. 310~318.

Lauffenburger, J. Ph., Basset, M., Coffin, F. and Gissinger, G. L., 2003, "Driver-Aid System Using Path-Planning for Lateral Vehicle Control," *Control Engineering Practice*, Vol. 11, No. 2, pp. 217~231.

Lee, B. J., Joo, Y. H. and Park, J. B., 2003, "An Intelligent Tracking Method for a Maneuvering Target," *International Journal of Control, Automation, and Systems*, Vol. 1, No. 1, pp. 93~100.

Lee, C. K. and Yi, K. S., 2002, "An Investigation of Vehicle-to-Vehicle Distance Control Laws Using Hardware-in-the Loop Simulation," (in Korean), *Transactions of the KSME, A*, Vol. 26, No. 7, pp. 1401~1407.

Lee, I. S., Lee, Y. H., Son, Y. D. and Moon, D. Y., 2002, "Vehicle Navigation Using Carrier Phase of GPS/GLONASS," (in Korean), *Journal of Korean Navigation and Port Research*, Vol. 26, No. 3, pp. 303~309.

Lee, T. G., 2003, "Centralized Kalman Filter with Adaptive Measurement Fusion: Its Application to a GPS/SDINS Integration System with an Additional Sensor," *International Journal of Control, Automation, and Systems*, Vol. 1, No. 4, pp. 444~452.

Lee, Y. H., Park, E. K., Park, T. J., Ryu, K. R. and Kim, K. H., 2003, "AGV System Operating Scheme Based on Grid Level Control in Automated Terminal," (in Korean), *Journal of Korean Navigation and Port Research*, Vol. 27, No. 2, pp. 223~231.

Li, X. and Bar-Shalom, Y., 1996, "Multiple-Model Estimation with Variable Structure," *IEEE Transactions on Automatic Control*, Vol. 41, No. 4, pp. 478~493.

Li, X. and Bar-Shalom, Y., 1993, "Design of

an Interacting Multiple Model Algorithm for Air Traffic Control Tracking," *IEEE Transactions on Control Systems Technology*, Vol. 1, No. 3, pp. 186~194.

Lim, J. H. and Kang, C. U., 2002, "Grid-Based Localization of a Mobile Robot Using Sonar Sensors," *KSME International Journal*, Vol. 16, No. 3, pp. 302~309.

Madhavan, R. and Durrant-Whyte, H. F., 2004, "Natural Landmark-Based Autonomous Vehicle Navigation," *Robotics and Autonomous Systems*, Vol. 46, pp. 79~95.

Mazor, E., Averbuch, A., Bar-Shalom, Y. and Dayan, J., 1998, "Interacting Multiple Model Methods in Target Tracking: A Survey," *IEEE Transactions on Aerospace and Electronic Systems*, Vol. 34, No. 1, pp. 103~123.

McGinnity, S. and Irwin, G. W., 1998, "Fuzzy Logic Approach to Manoeuvring Target Tracking," *IEE Proceedings on Radar, Sonar, and Navigation*, Vol. 145, No. 6, pp. 337~341.

Moon, I. K. and Yi, K. S., 2002, "Vehicle Tests of a Longitudinal Control Law for Application to Stop-and-Go Cruise Control," *KSME International Journal*, Vol. 16, No. 9, pp. 1166~1174.

Munir, A. and Atherton, D. P., 1995, "Adaptive Interacting Multiple Model Algorithm for Tracking a Manoeuvring Target," *IEE Proceedings on Radar, Sonar, and Navigation*, Vol. 142, No. 1, pp. 11~17.

Nabaa, N. and Bishop, R. H., 2000, "Validation and Comparison of Coordinated Turn Aircraft Maneuver Models," *IEEE Transactions on Aerospace and Electronic Systems*, Vol. 36, No. 1, pp. 250~259.

Park, T. J., Ahn, J. W. and Han, C. S., 2002, "A Path Generation Algorithm of an Automatic Guided Vehicle Using Sensor Scanning Method," *KSME International Journal*, Vol. 16, No. 2, pp. 137~146.

Rajamani, R., Zhu, C. and Alexander, L., 2003, "Lateral Control of a Backward Driven Font-Steering Vehicle," *Control Engineering Practice*, Vol. 11, No. 5, pp. 531~540.

Ristic, B. and Arulampalam, M. S., 2003, "Tracking a Manoeuvring Target Using Angle-Only Measurements: Algorithms and Performance," *Signal Processing*, Vol. 83, No. 6, pp. 1223~1238.

Semerdjiev, E. and Mihaylova, L., 2000, "Variable- and Fixed-Structure Augmented Interacting Multiple-Model Algorithms for Manoeuvring Ship Tracking Based on New Ship Models," *International Journal of Applied Mathematics and Computer Science*, Vol. 10, No. 3, pp. 591~604.

Simeonova, I. and Semerdjiev, T., 2002, "Specific Features of IMM Tracking Filter Design," *An International Journal of Information and Security*, Vol. 9, pp. 154~165.

Tam, W. I., Plataniotis, K. N. and Hatzinakos, D., 1999, "An Adaptive Gaussian Sum Algorithm for Radar Tracking," *Signal Processing*, Vol. 77, No. 1, pp. 85~104.

Togneri, R., Ma, J. and Deng, L., 2001, "Parameter Estimation of a Target-Directed Dynamic System Model with Switching States," *Signal Processing*, Vol. 81, No. 5, pp. 975~987.

Xu, F., Brussel, H. V., Nuttin, M. and Moreas, R., 2003, "Concepts for Dynamic Avoidance and Their Extended Application in Underground Navigation," *Robotics and Autonomous Systems*, Vol. 42, No. 1, pp. 1~15.

Zhang, W. W., Zhuang, B. H. and Zhang, Y., 2000, "Novel Navigation Sensor for Autonomous Guide," *Optical Engineering*, Vol. 39, No. 9, pp. 2511~2516.